

Size effects in twinned nanopillars

Farah Hammami and Yashashree Kulkarni

Citation: *Journal of Applied Physics* **116**, 033512 (2014); doi: 10.1063/1.4890541

View online: <http://dx.doi.org/10.1063/1.4890541>

View Table of Contents: <http://scitation.aip.org/content/aip/journal/jap/116/3?ver=pdfcov>

Published by the [AIP Publishing](#)

Articles you may be interested in

[Size effects of primary/secondary twins on the atomistic deformation mechanisms in hierarchically nanotwinned metals](#)

J. Appl. Phys. **113**, 203516 (2013); 10.1063/1.4808096

[Atomistic investigation of scratching-induced deformation twinning in nanocrystalline Cu](#)

J. Appl. Phys. **112**, 073526 (2012); 10.1063/1.4757937

[Molecular dynamics simulation of Bauschinger's effect in deformed copper single crystal in different strain ranges](#)

J. Appl. Phys. **110**, 124911 (2011); 10.1063/1.3672414

[Structure and migration of \(112\) step on \(111\) twin boundaries in nanocrystalline copper](#)

J. Appl. Phys. **104**, 113717 (2008); 10.1063/1.3035944

[Strain hardening and large tensile elongation in ultrahigh-strength nano-twinned copper](#)

Appl. Phys. Lett. **85**, 4932 (2004); 10.1063/1.1814431



AIP | Journal of
Applied Physics

Journal of Applied Physics is pleased to
announce **André Anders** as its new Editor-in-Chief

Size effects in twinned nanopillars

Farah Hammami and Yashashree Kulkarni^{a)}

Department of Mechanical Engineering, University of Houston, Houston, Texas 77204, USA

(Received 30 April 2014; accepted 6 July 2014; published online 18 July 2014)

Nanotwinned structures are becoming increasingly attractive owing to their potential as optimal motifs for strength, ductility, and grain stability in metals. In this work, we use nanopillar compression as a paradigmatic problem to investigate the interplay between size effects associated with the twin spacing and the finite size of the nanopillars by way of molecular dynamics simulations. Our simulations reveal that the aspect ratio plays an important role in governing the weakening or strengthening effect of coherent twin boundaries under uniaxial compression. We find that there exists an optimal aspect ratio for which the yield strength of twinned nanopillars is slightly higher than even single crystal nanopillars. In addition, we observe that twin boundaries facilitate dislocation-starvation as defects glide along twin boundaries and are eliminated at the free surface. © 2014 AIP Publishing LLC. [<http://dx.doi.org/10.1063/1.4890541>]

I. INTRODUCTION

It has long been known that mechanical properties scale dramatically with size, having important ramifications for the design of novel materials and technological development.¹ For instance, the nineties witnessed an intensity of research on nanocrystalline metals owing to their ultra-high strength that arises from the high density of grain boundaries serving as effective barriers for dislocation motion (see, e.g., Refs. 2–4). However, this early enthusiasm was met with severe disappointment due to their brittle nature and loss of structural stability that resulted from grain boundary-mediated processes and that offset other benefits of nanostructuring. In contrast, even more remarkable mechanical properties have been demonstrated by a special class of materials called the nanotwinned metals which comprise of microscale grains containing twins with lamella thickness on the order of less than hundred nanometers.^{5–8} The extraordinary strength and ductility of these materials is attributed to the presence of twin boundaries (TBs) that not only enhance the strength by serving as excellent barriers to dislocation motion but can accommodate large plastic strains by absorbing dislocations onto their twin planes, thereby enhancing ductility.^{9–14} Recent work has also demonstrated an intimate coupling between grain size and the critical TB spacing for maximum strengthening in nanotwinned structures.^{15,16} Thus, unlike nanocrystalline metals that exhibit high strength only at the expense of increased brittleness as well as susceptibility to grain growth, nanotwinned metals show great potential as optimal motifs for high strength, ductility, and stability, and hence have been the subject of active research in the past few years.

In this work, we study the role of TBs in the strengthening of twinned nanopillars under uniaxial compression via molecular dynamics simulations. Extensive experimental and computational studies on nanopillars have established that the sample geometry and size can have a significant effect on the mechanical properties especially at the micron

and sub-micron scales.^{18–27} In fact, the dramatic strengthening of single crystal nanopillars with decreasing sample size is attributed to a radical transition in the deformation mechanisms owing to the constrained volume and the presence of free surfaces. It has been demonstrated that the dominant strengthening mechanism at the nanoscale is dislocation starvation, as mobile dislocations can easily glide and exit the nanostructure from the free surfaces so that the plasticity is essentially governed by nucleation events.²⁹ Owing to the remarkable strengthening mechanisms enabled by twin boundaries as well as small sample dimensions of nanopillars, several studies have also probed the combined effect of the presence of TBs in nanopillars.^{30–36} While Afanasyev and Sansoz³⁰ examined the strengthening effect of TBs in cylindrical nanopillars under compression, Cao *et al.*³¹ investigated the role of TBs in nanopillars with square cross-section under tension. Both studies were performed by varying the twin spacing in a nanopillar of a specific diameter. Zhang and Huang³² showed that surface morphologies can also lead to a strengthening or softening effect of TBs on nanopillar compression. In their tensile simulations of twinned nanowires, Deng and Sansoz^{33–35} observed that the strengthening or weakening effect of TBs under tension is a function of the twin spacing as well as the pillar diameter. They report a critical ratio of diameter to twin spacing at which a transition in plasticity mechanism occurs. Through a combined experimental and computational study, Jang *et al.*³⁶ recently revealed a strong effect of the TB spacing as well as twin orientation on the yield strength and failure of nanotwinned nanopillars under tension. Complementing the insights gained through these atomistic studies, we investigate the interplay of the size effects in twinned nanopillars under uniaxial compression associated with the twin spacing and the sample size. We refer to the TB spacing as the intrinsic dimension and the pillar diameter as the extrinsic dimension. We use nanopillar compression as a paradigmatic problem to elucidate the deformation mechanisms arising from the interplay of these two specific size effects owing to the presence of both TBs and free surfaces. Since nanowires exhibit considerably distinct behavior under tension and

^{a)}Electronic mail: ykulkarni@uh.edu

compression,¹⁷ we also examine the existence of an optimal ratio of the TB spacing and the pillar diameter for strengthening and report our findings within the context of the previous studies on twinned nanopillars and nanowires, which have been mostly performed under tension.

II. SIMULATION METHOD

The response of single crystal and twinned nanopillar specimens under compression was studied via molecular dynamics simulations using LAMMPS.³⁷ The simulations were performed at zero temperature under the canonical (NVT) ensemble using the embedded-atom method (EAM) potential for Cu developed by Mishin *et al.*³⁸ Fig. 1 shows the crystallographic orientation of the pillars with the axis aligned along the [111] direction, and the lateral (x and y) coordinate axes oriented along the $[\bar{1}\bar{1}2]$ and the $[1\bar{1}0]$ directions, respectively. The coherent twin boundaries (CTBs) were aligned normal to the z-direction. The nanopillars had circular cross-sections with diameters ranging from 6 nm to 15 nm and height maintained constant at 25 nm. Depending on the specimen size, the number of atoms ranged from 58 000 to 400 000 atoms. Table I summarizes the details of the specimen sizes considered. For the twinned specimen, seven different TB spacings were examined. They consisted of 2, 4, 6, 8, 10, 12, and 19 CTBs corresponding to twin spacings of 8.3, 5, 3.6, 2.8, 2.3, 1.92, and 1.25 nm, respectively. Table II summarizes these details of the twinned specimens. The nanopillars were non-periodic in the axial direction and had free surface boundary conditions in the lateral directions. Equilibration of the samples was achieved by conjugate gradient energy minimization followed by NVT relaxation for 50 ps. Compression was performed by fixing a few layers of atoms at the bottom and displacing a few layers of atoms at the top by increments of -0.64 \AA along the $[1\ 1\ 1]$ direction. The specimen was relaxed between each increment of

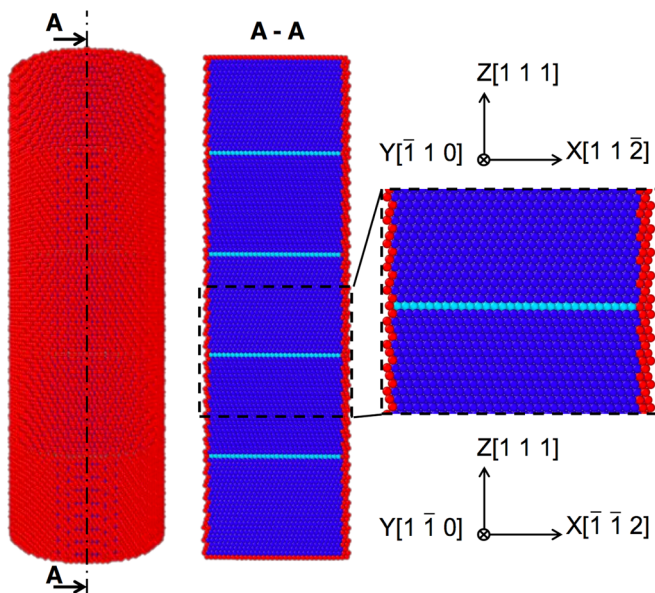


FIG. 1. Atomistic view of the nanopillar specimen of Cu with $\Sigma 3(111)$ coherent twin boundaries used in this study. Atoms are colored according to the centrosymmetry values.

TABLE I. Configurations of nanopillars with different diameters (D) and heights (H) considered in this study.

Specimen	D (nm)	H (nm)	Number of Atoms	Aspect Ratio
D6	6	25	58,360	4
D8	8	25	114,280	3
D12	12	25	232,600	2
D15	15	25	392,200	1.67

TABLE II. Various configurations of nanopillars with twin boundaries considered in this study (X refers to the diameter that can be 6, 8, 12, or 15 (nm)).

Specimen	Number of CTBs	CTB spacing (nm)
DXTB2	2	8.3
DXTB4	4	5
DXTB6	6	3.6
DXTB8	8	2.8
DXTB10	10	2.3
DXTB12	12	1.92
DXTB19	19	1.25

displacement for 25 ps. Thus, the average strain rate was about $1.1 \times 10^8 \text{ s}^{-1}$. The virial stress and strain along the loading direction were calculated at the end of the relaxation after each increment of displacement. The defect structures were visualized in OVITO³⁹ using the centrosymmetry parameter.⁴⁰

III. RESULTS AND DISCUSSION

Fig. 2 shows a typical stress-strain curve obtained for most of our specimens under uniaxial compression. The Young's modulus is observed to be about 170 GPa for single crystal as well as twinned specimen, which is consistent with literature.^{28,31} We note that most of the molecular studies available in literature focus on Au and involve tension simulations. Due to the significant tension-compression asymmetry observed in nanowires¹⁷ and fundamentally distinct mechanical response of different fcc metals,³⁵ it is difficult

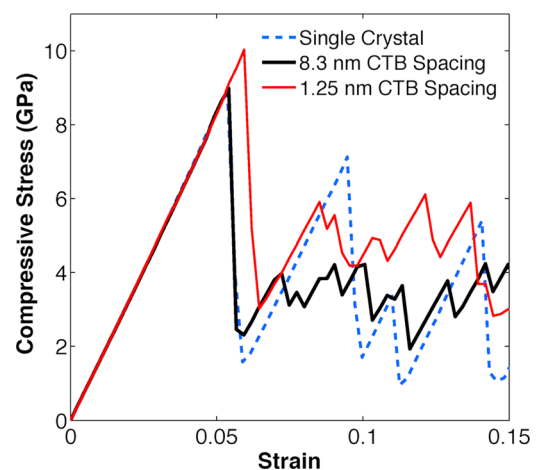


FIG. 2. Stress versus strain curves for Cu single crystal, 8.3 nm TB spacing and 1.25 nm TB spacing nanopillars with 8 nm diameter at 0 K.

to compare our results directly with those available in literature. Hence, we have verified our simulation codes by reproducing the tension simulations of Cao *et al.*³¹ for a Cu nanowire of square cross-section, and the compression simulations of Afanasyev and Sansoz³⁰ for a Au nanopillar of circular cross-section. Fig. 2 shows that the single crystal nanopillar exhibits larger serrations compared to the twinned nanopillars. This is due to the fact that the dislocations nucleated during the previous drop in the curve glide along their slip planes and are eliminated at the free surface. Consequently, the specimen becomes defect-free again and shows a subsequent elastic response.³⁰ In the case of twinned pillars, the stress-strain curve is primarily dominated by multiple boundary-mediated processes such as pile up of dislocations at the CTBs, and their absorption and glide on the twin planes. The yield strengths of all the specimens are compiled in Fig. 3. The solid curves represent the variation of the yield strength with twin boundary spacing for pillars with different diameters. The dashed lines represent the yield strength of corresponding single crystal nanopillars of the same diameter. Here, the yield stress represents the stress value that corresponds to the first drop in the stress-strain curve, as shown in the example in Fig. 2, indicating the onset of plasticity with the first dislocation nucleation event.

Although our focus is on twinned nanopillars, we first briefly discuss the effect of the extrinsic dimension, that is the pillar diameter, on the yield strength of a nanopillar. As seen in Fig. 3, the yield stress of single crystal nanopillars exhibits a strong size-dependence. In agreement with prior theoretical and experimental studies, the strength increases with decreasing diameter.^{18–20,24,41} Plasticity is found to initiate with dislocations nucleating from the surface of the cylindrical specimen. The size-dependence of the yield stress is attributed to the fact that the critical stress for dislocation nucleation at the surface also scales with the pillar diameter due to the constrained volume offered by the smaller pillars that makes it harder for the dislocations to nucleate.^{19,24} Fig. 4 shows the evolution of the defect structure in the single crystal

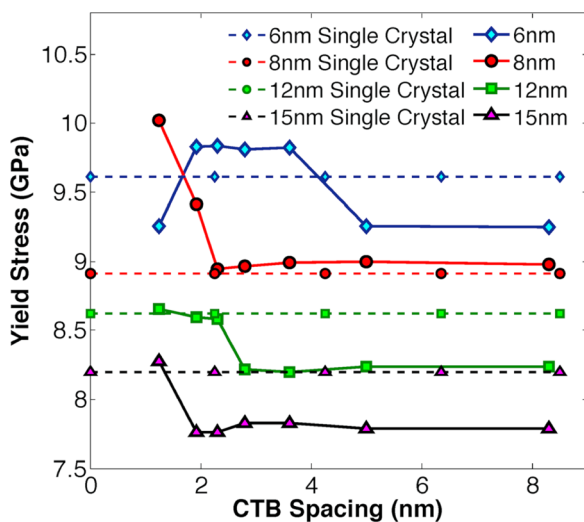


FIG. 3. Yield strength versus coherent twin boundary spacing for different nanopillar diameters. The yield strength for the corresponding single crystal nanopillars is shown by a dashed line.

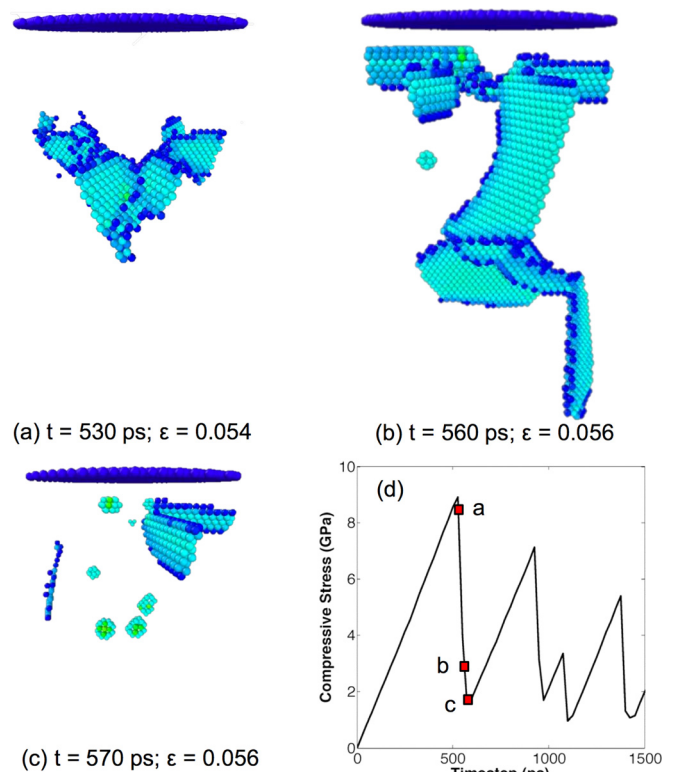


FIG. 4. Evolution of the defect structure in specimen D8 during compression. The snapshots (a)–(c) are zoomed in views of the nanopillar showing the dislocation structure. The top surface is shown for reference. The stress versus time plot (d) indicates the instants at which the snapshots (a)–(c) were taken.

nanopillar with 8 nm diameter during uniaxial compression. Partial dislocations are first emitted from the surface leading to a complex intersection of stacking faults. Multiple $\{111\}$ slip systems are activated possibly due to the high stresses in the specimen as the simulations were performed at zero temperature. The partial dislocations then glide along their slip planes and are rapidly eliminated at the surface leaving behind surface steps and some residue in the interior of the specimen. On continued compression, these residual defects become sources for further dislocation activity.

An intriguing behavior is observed on comparing the yield strength of nanopillars with and without twins. In Fig. 3, all nanopillars, except the one with 8 nm diameter, show substantial decrease of over 0.5 GPa in the yield stress after the introduction of twin boundaries. Only the pillar with a diameter of 8 nm exhibits a slightly higher yield strength with CTBs than the corresponding single crystal nanopillar. It is rather surprising that the introduction of CTBs has such contrasting effects on nanopillars with different diameters and indicates the possibility of optimal specimen dimensions for the strengthening effect of CTBs. This trend observed in our simulations of uniaxial compression has not been reported in literature before. For instance, Cao *et al.*³¹ considered Cu nanopillars with a square cross-section under tension and observed a higher yield strength even with one TB as compared to a single crystal nanopillar. In contrast, Hyde *et al.*²¹ observed the TBs to weaken the nanowires. Zhang and Huang³² found that TBs strengthen nanopillars with square

cross-section, but might soften those with circular cross-section. However, Afanasyev and Sansoz³⁰ considered a cylindrical Au nanopillar of 12 nm diameter under compression and observed the twinned nanopillars to have a higher yield strength than the single crystal counterpart. For Au nanowires under tension, Deng and Sansoz³³ found that there exists a transition from twin weakening to twin strengthening for the nanowire diameters they considered.

In order to reconcile our simulation results with these different studies, we first note that the 8 nm pillar considered in our study has an aspect ratio of 3, similar to the specimen considered by Afanasyev and Sansoz³⁰ that showed TB strengthening. To examine the possible role of aspect ratio, we repeated the uniaxial compression tests on nanopillars of different diameters but maintaining the aspect ratio of about 3. Fig. 5 shows the yield stress for the three different pillars of diameters 6 nm, 8 nm, and 12 nm considered. In contrast with the results shown in Fig. 3, all pillars now show a mild increase in the yield stress with CTBs compared to the single crystal nanopillar of the same diameter. We performed additional simulations considering different aspect ratio for nanopillar heights ranging from 18 nm to 36 nm. The results are compiled in Fig. 6. In fact, for the specimen with 36 nm height, we considered diameters ranging from 8–21 nm leading to aspect ratio ranging from 4.5–1.7. These specimens with a height of 36 nm show the same trend as that shown by the specimen with a height of 25 nm. This clearly indicates that the aspect ratio, and not just the pillar diameter, plays a role in strengthening or weakening a nanopillar with CTBs when compared to the corresponding single crystal nanopillars. There is an optimal range of length to diameter ratio between 2.5 to 3.2 at which the twinned nanopillars have higher or almost the same yield strength as their single crystalline counterparts.

We now examine the effect of the CTB spacing on the yield strength of a nanopillar. We find that under uniaxial

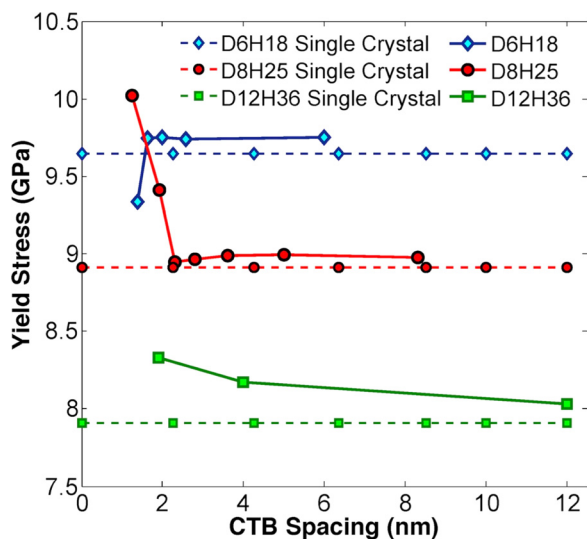


FIG. 5. Compressive yield stress versus twin boundary spacing for pillars with different diameters but same aspect ratio of 3:1. The yield strength for corresponding single crystal nanopillars are shown by dashed lines. D6H18, D8H25, and D12H36 represent nanopillars with diameters 6 nm, 8 nm, and 12 nm and heights 18 nm, 25 nm, and 36 nm, respectively.

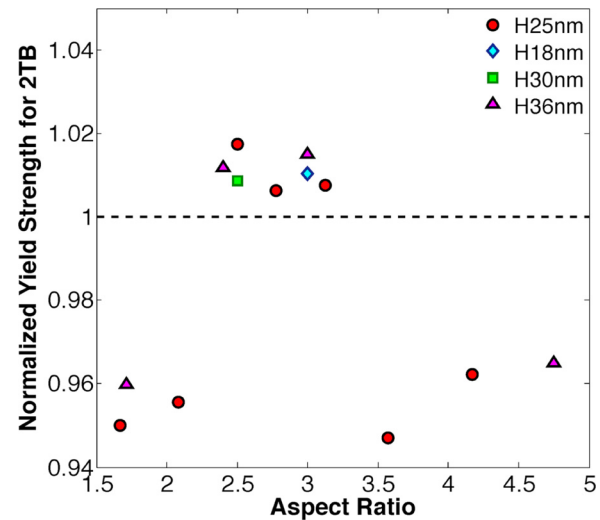


FIG. 6. The yield strength of nanopillars with two CTBs normalized with the yield strength of the single crystal nanopillar of the same diameter and plotted against the height to diameter ratio of the nanopillars. The different shapes (triangles, circles, squares) indicate specimen with different height as specified in the legend.

compression this dependence is surprisingly weak. As seen in Fig. 3, the yield stress for all nanopillars remains steady as CTB spacing is decreased from 8.3 nm (corresponding to 2 CTBs). Only when the CTB spacing reduces to about 2 nm, the yield stress shows a dramatic increase of almost 0.5 GPa. In fact, the pillar with the largest diameter (15 nm) shows an increase in yield strength only when the twin lamellar thickness reaches 1.25 nm, whereas the one with the smallest diameter (6 nm) shows an increase in yield strength with twin lamellar thickness of about 4 nm. However, at about 1.92 nm CTB spacing, the yield stress of the 6 nm pillar drops abruptly. This decrease is due to the combination of extremely small intrinsic and extrinsic dimensions as the large number of CTB-surface junctions offers more nucleation sites for defects. Thus, generally speaking, we can conclude that the yield strength tends to increase at lower TB density (or larger TB spacing) for decreasing pillar diameters. In other words, pillars with larger diameters require greater twin density to enhance the strengthening effect of twin boundaries. Comparison of the yield strength of twinned specimens with the same aspect ratio (as in Fig. 5) also shows similar trends. In Fig. 5, the thickest nanopillar with 12 nm diameter exhibits a gradual increase in yield stress with decreasing CTB spacing. This is in agreement with the response of the nanopillar considered by Afanasyev and Sansoz³⁰ with the same dimensions. However, the thinnest (6 nm) pillar now does not show any strengthening with decreasing TB spacing, but still shows the abrupt drop at 1.92 nm spacing. Although we do not fully understand the atomistic mechanisms leading to these detailed differences in Figs. 3 and 5, our overall prediction is that nanopillars with diameters 8 nm and larger exhibit a dramatic increase in yield strength when CTB spacings become extremely small, on the order of a nanometer or less. This is also consistent with the recent work by Jang *et al.*³⁶ and Wang *et al.*⁴² Their experimental and computational studies reveal very high

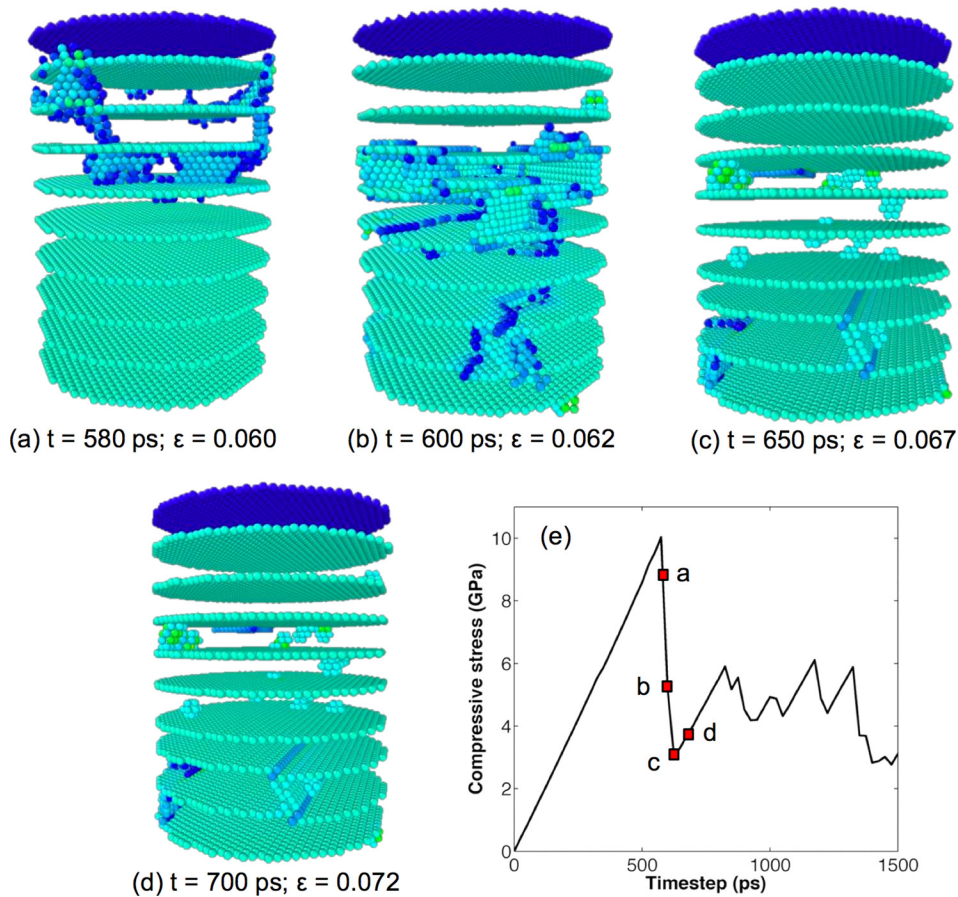


FIG. 7. Evolution of the defect structure in specimen D8TB19 during compression. The snapshots (a)–(d) are zoomed in views of the nanopillar showing the dislocation structure. The stress versus time plot (e) indicates the instants at which the snapshots (a)–(d) were taken.

strength of nanowires containing ultra-high density of twins resulting from angstrom-scale TB spacing. Fig. 7 shows the evolution of the defect structure in specimen D8TB19 during the compression simulation. We note that the partial dislocations first nucleate from the free surface leading to a pile-up of dislocations at the CTBs. The dislocations are then absorbed onto the $\{111\}$ twin planes and can easily glide along the CTB whereas some can be transmitted into the adjacent twin. The dislocations are finally eliminated at the free surface leaving the nanopillar with fewer defects and consequently with enhanced strength. Thus, we conclude that the strengthening mechanism is a combination of dislocation pile-up at CTBs and dislocation-starvation as CTBs provide additional routes for dislocations to rapidly reach the free surface and be annihilated.

IV. CONCLUSION

In summary, we have performed molecular dynamics simulations of uniaxial compression on twinned nanopillars to elucidate the interplay of intrinsic and extrinsic size-scale effects on the strengthening mechanisms. An intriguing revelation is that there is an optimal aspect ratio for which the yield strength of twinned nanopillars is higher than even single crystal nanopillars, in contrast to other aspect ratio for which the yield strength of twinned nanopillars is considerably lower than their single crystalline counterparts. The atomistic origins of this behavior are not yet clear to us. Further theoretical and experimental studies are needed to shed light

on the role of the aspect ratio on the strengthening or weakening effect of twin boundaries in nanopillars. Another interesting observation is that the yield strength of the twinned nanopillars continues to increase dramatically even when the twin boundary spacing is reduced to the order of angstroms. This is in sharp contrast to conventional (polycrystalline) nanotwinned metals which exhibit a loss of strength as twin lamella thickness is reduced below 10–15 nm.^{8,15,16} However, our observations are consistent with recent experimental and computational studies on nanopillars and nanowires with ultra-high density of twins.^{36,42} Even at these extremely small, angstrom-scale twin boundary spacings, the CTBs enhance the strength by arresting dislocation motion and eventually serving as channels for dislocations to glide and annihilate at the free surface. We note that the effect of the aspect ratio observed in the case of CTBs may often be dominated by other competing mechanisms. For instance, incoherent TBs and defective CTBs may exhibit plasticity mechanisms very different from those reported here thereby affecting the role of the aspect ratio and hence warrant further examination through experiments and computations. Similarly, it would also be insightful to investigate the role of the orientation of the CTBs with respect to the loading direction as well as temperature on these deformation mechanisms. In light of the recent work revealing the attractive mechanical properties of nanoporous nanotwinned copper,⁴³ it would also be interesting to elucidate the role of twin boundaries on the strength and stability of these structures from atomistic simulations. Thus, the interplay of strengthening mechanisms in twinned

nanopillars can open further avenues for the design of novel nanotwinned structures as optimal motifs for next-generation structural applications.

ACKNOWLEDGMENTS

The authors would like to acknowledge the support of the US National Science Foundation under grants DMR-1006876. The simulations were partly performed on the supercomputing facility hosted by the Research Computing Center at University of Houston.

- ¹T. Zhu, J. Li, S. Ogata, and S. Yip, *MRS Bull.* **34**, 167 (2009).
- ²H. Gleiter, *Prog. Mater. Sci.* **33**, 223 (1989).
- ³H. Van Swygenhoven, *Science* **296**, 66 (2002).
- ⁴M. Dao, L. Lu, R. J. Asaro, J. T. M. De Hosson, and E. Ma, *Acta Mater.* **55**, 4041 (2007).
- ⁵L. Lu, Y. Shen, X. Chen, L. Qian, and K. Lu, *Science* **304**, 422 (2004).
- ⁶X. Zhang, H. Wang, X. H. Chen, L. Lu, K. Lu, R. G. Hoagland, and A. Misra, *Appl. Phys. Lett.* **88**, 173116 (2006).
- ⁷A. M. Hodge, Y. M. Wang, and T. W. Barbee, Jr., *Scr. Mater.* **59**, 163 (2008).
- ⁸K. Lu, L. Lu, and S. Suresh, *Science* **324**, 349 (2009).
- ⁹M. Dao, L. Lu, Y. F. Shen, and S. Suresh, *Acta Mater.* **54**, 5421 (2006).
- ¹⁰T. Zhu, J. Li, A. Samanta, H. G. Kim, and S. Suresh, *Proc. Natl. Acad. Sci., U.S.A.* **104**, 3031 (2007).
- ¹¹Z. X. Wu, Y. W. Zhang, and D. J. Srolovitz, *Acta Mater.* **57**, 4508 (2009).
- ¹²R. J. Asaro and Y. Kulkarni, *Scr. Mater.* **58**, 389 (2008).
- ¹³Y. Kulkarni and R. J. Asaro, *Acta Mater.* **57**, 4835 (2009).
- ¹⁴H. Mirkhani and S. P. Joshi, *J. Mech. Phys. Solids* **68**, 107 (2014).
- ¹⁵X. Li, Y. Wei, L. Lu, K. Lu, and H. Gao, *Nature* **464**, 877 (2010).
- ¹⁶Y. Wei, *Phys. Rev. B* **83**, 132104 (2011).
- ¹⁷J. Diao, K. Gall, and M. L. Dunn, *Nano Lett.* **4**, 1863 (2004).
- ¹⁸M. D. Uchic, D. M. Dimiduk, J. N. Florando, and W. D. Nix, *Science* **305**, 986 (2004).
- ¹⁹V. S. Deshpande, A. Needleman, and E. Van der Giessen, *J. Mech. Phys. Solids* **53**, 2661 (2005).
- ²⁰J. R. Greer and W. D. Nix, *Appl. Phys. A* **80**, 1625 (2005).
- ²¹B. Hyde, H. D. Espinosa, and D. Farkas, *JOM* **57**, 62 (2005).
- ²²E. Rabkin and D. J. Srolovitz, *Nano Lett.* **7**, 101 (2007).
- ²³A. Cao and E. Ma, *Acta Mater.* **56**, 4816 (2008).
- ²⁴C. R. Weinberger and W. Cai, *Proc. Natl. Acad. Sci., U.S.A.* **105**, 14304 (2008).
- ²⁵M. D. Uchic, P. A. Shade, and D. M. Dimiduk, *Annu. Rev. Mater. Res.* **39**, 361 (2009).
- ²⁶J. A. Brown and N. M. Ghoniem, *Acta Mater.* **58**, 886 (2010).
- ²⁷R. J. Milne, A. J. Lockwood, and B. J. Inkson, *J. Phys. D* **44**, 1 (2011).
- ²⁸Z. X. Wu, Y. W. Zhang, M. H. Jhon, J. R. Greer, and D. J. Srolovitz, *Acta Mater.* **61**, 1831 (2013).
- ²⁹J. R. Greer and W. D. Nix, *Phys. Rev. B* **73**, 245410 (2006).
- ³⁰K. A. Afanasyev and F. Sansoz, *Nano Lett.* **7**, 2056 (2007).
- ³¹A. J. Cao, Y. G. Wei, and S. X. Mao, *Appl. Phys. Lett.* **90**, 151909 (2007).
- ³²Y. Zhang and H. Huang, *Nanoscale Res. Lett.* **4**, 34 (2009).
- ³³C. Deng and F. Sansoz, *Appl. Phys. Lett.* **95**, 091914 (2009).
- ³⁴C. Deng and F. Sansoz, *Nano Lett.* **9**, 1517 (2009).
- ³⁵C. Deng and F. Sansoz, *Acta Mater.* **57**, 6090 (2009).
- ³⁶D. Jang, X. Li, H. Gao, and J. R. Greer, *Nat. Nanotechnol.* **7**, 594 (2012).
- ³⁷S. J. Plimpton, *J. Comput. Phys.* **117**, 1 (1995).
- ³⁸Y. Mishin, M. J. Mehl, D. A. Papaconstantopoulos, A. F. Voter, and J. D. Kress, *Phys. Rev. B* **63**, 224106 (2001).
- ³⁹A. Stukowski, *Modell. Simul. Mater. Sci. Eng.* **18**, 015012 (2010).
- ⁴⁰C. L. Kelchner, S. J. Plimpton, and J. C. Hamilton, *Phys. Rev. B* **58**, 11085 (1998).
- ⁴¹L. Zuo, A. H. W. Ngan, and G. P. Zheng, *Phys. Rev. Lett.* **94**, 095501 (2005).
- ⁴²J. Wang, F. Sansoz, J. Huang, Y. Liu, S. Sun, Z. Zhang, and S. X. Mao, *Nat. Commun.* **2768**, 1 (2013).
- ⁴³R. Liu, S. Zheng, J. K. Baldwin, M. Kuthuru, N. Mara, and A. Antoniou, *Appl. Phys. Lett.* **103**, 241907 (2013).